



UNIVERSITI PUTRA MALAYSIA

***THE INFLUENCE OF MICROSTRUCTURE EVOLUTION ON THE
DIELECTRIC PROPERTIES OF
STRONTIUM TITANATE AND ALUMINA SILICATE***

LEOW CHUN YAN

FS 2015 60



**THE INFLUENCE OF MICROSTRUCTURE EVOLUTION ON
THE DIELECTRIC PROPERTIES OF
STRONTIUM TITANATE AND ALUMINA SILICATE**

By

LEOW CHUN YAN

**Thesis Submitted to the School of Graduate Studies, Universiti Putra
Malaysia, in Fulfilment of the Requirements for the Degree of Degree of
Master of Science**

May 2015

All material contained within the thesis, including without limitation text, logos, icons, photographs and all other artwork, is copyright material of Universiti Putra Malaysia unless otherwise stated. Use may be made of any material contained within the thesis for non-commercial purposes from the copyright holder. Commercial use of material may only be made with the express, prior, written permission of Universiti Putra Malaysia.

Copyright © Universiti Putra Malaysia



Abstract of thesis presented to the Senate of Universiti Putra Malaysia in fulfilment of the requirement for the degree of Master of Science

**THE INFLUENCE OF MICROSTRUCTURE EVOLUTION ON
THE DIELECTRIC PROPERTIES OF
STRONTIUM TITANATE AND ALUMINA SILICATE.**

By

LEOW CHUN YAN

May 2015

Chair: Jumiah Hassan, PhD

Faculty: Science

Strontium Titanate (ST) and Alumina Silicate (AS) have wide range of applications as an advance ceramics. They are well known for their reliable performance especially at high temperature applications. Due to their amazing properties, most of the studies often focus on the after formation of its crystal structure phase and microstructure changes towards the dielectric properties. In fact, these studies are lacks of information link with the early stage of synthesis process. Wide range of sintering temperature and different particle size of green body must be set, in order to have a better understanding on the properties of ST and AS.

In this study, a series of these samples were prepared by conventional solid-state reaction method with two different particle sizes (sieved with laboratory test sieve of size 45 μm and 20 μm). These samples undergo a sintering process at temperatures from 500°C to 1400°C at 100°C intervals. Across this sintering temperature range. Average grain size of the samples were measured to investigate the microstructure evolution. Field Emission Scanning Electron Microscopy (FESEM) was carried out to capture samples microscopic images while X-ray diffraction (XRD) analysis was to study and confirmed the formation of crystal structure phase of ST and AS. Average grain size changes and crystal structure formation were studied in parallel with the dielectric properties at various measuring temperatures. Dielectric properties of ST and AS were analyzed at two different frequency range. For low frequency dielectric measurement, the frequency range is at 40 Hz – 1 MHz at measuring temperature from 28°C to 300°C with 50°C interval. For microwave dielectric measurements, the frequency range is at 1 MHz – 1.8 GHz at room temperature.

Based on XRD analysis, ST crystal structure started to form at 700°C sintering temperature. Synthesis was complete at 900°C. For AS, mullite compound was found and confirmed by XRD analysis at 1300°C and 1400°C sintering temperature. By observation, microstructure of ST started from agglomerated powder to form grains. As sintering temperature increases, grains continue to grow through the necking process. The evolution process is almost completed when grain boundaries diffuse with each other to form larger grains. By comparing both series of ST samples sintered at 1400°C, average grain size of the sample with greater starting particles size is 0.640 μm while another is 0.496 μm . ST45 (sieved with test sieve of 45 μm) was experiencing rapid grain growth at the final sintering stage, while ST20 (sieved with test sieve of 20 μm) grain growth was slower. For AS, thin and long rectangular shape grain structure were observed in samples sintered at 1400°C. ST samples with greater starting particles size form larger grain size.

At low frequency measurement, dielectric constant is dependent on frequency. Grain size will alter the dielectric constant of ST depending on the measuring temperatures. Loss tangent, $\tan \delta$ is also dependent on measuring temperature. Loss peak are strongly connected with frequency and measuring temperature. Agglomerations of powders will encourage alternating current conduction at high measuring temperature and causing the dielectric constant to drop. Dielectric constant of ST20 is greater than ST45 due to greater interfacial polarization effects occurred in ST20. ST20 has smaller grain size that would increase its surface effect. Rapid grain growth in ST45 had reduces its dielectric properties performances. Slower grain growth is important to promote homogeneous grain size and grains distribution during ST microstructure evolution. Homogeneous and smaller particle size are important factors to form high quality ST ceramic with good dielectric properties. For microwave frequency measurement, when frequency is beyond 10^7 Hz, dielectric constant value will remains constant across increasing frequency. Dielectric properties of ST is dependent of the grain size. ST with complete crystal structure will show greater dielectric constant value.

Abstrak tesis yang dikemukakan kepada Senat Universiti Putra Malaysia sebagai memenuhi keperluan untuk ijazah Master Sains

PENGARUHAN EVOLUSI MIKROSTRUKTUR PADA SIFAT-SIFAT DIELEKTRIK BAGI STRONTIUM TITANAT DAN ALUMINA SILIKAL

Oleh

LEOW CHUN YAN

Mei 2015

Pengerusi: Jumiah Hassan, PhD

Fakulti: Sains

Strontium Titanat (ST) dan Alumina Silikal (AS) mempunyai pelbagai aplikasi sebagai seramik mara. Ia terkenal dengan prestasi mantap terutamanya dalam aplikasi suhu tinggi. Berdasarkan sifat-sifat mereka yang menakjubkan, kebanyakan penyelidikan selalu menumpu pada selepas pembentukan fasa struktur kristal dan perubahan mikrostruktur terhadap sifat dielektrik. Sebenarnya, penyelidikan-penyelidikan ini kekurangan maklumat berhubung dengan proses sintesis pada tahap awal. Suhu dengan jarak yang luas dan pelbagai saiz zarah badan hijau mesti ditetapkan untuk pemahaman yang lebih baik terhadap sifat-sifat ST dan AS.

Dalam kajian ini, sesiri sampel telah disediakan dengan kaedah reaksi konvensional keadaan pepejal dengan saiz zarah yang berbeza (disaring dengan ayak makmal ujian saiz 45 μm and 20 μm). Sample ini akan melalui proses penyepuhlingapan dari suhu 500°C ke 1400°C selang 100°C. Melalui jarak suhu penyepuhlingapan ini, purata saiz bijiran sampel telah diukur demi menyelidik evolusi mikrostruktur. Perlepasan medan mikroskop elektron imbasan (FESEM) telah dijalankan untuk mengambil imej mikroskopik sampel manakala pembelauan sinar-X (XRD) analisis adalah untuk mengkaji dan mengesahkan pembentukan fasa struktur kristal pada ST dan AS. Perubahan purata saiz bijiran dan pembentukan struktur kristal telah dikaji selari dengan sifat dielektrik pada suhu pengukuran yang berbeza. Sifat dielektrik bagi ST dan AS telah dianalisis pada jarak frekuensi yang berlainan. Untuk ukuran dielektrik frekuensi rendah, jarak frekuensi terletak pada 40 Hz – 1 MHz dengan suhu pengukuran dari 28°C to 300°C selang 50°C. Manakala bagi ukuran dielektrik gelombangmikro, jarak frekuensi terletak pada 1 MHz – 1.8 GHz dalam suhu bilik.

Berdasarkan XRD analisis, struktur kristal ST mula membentuk pada 700°C suhu penyepuhlingapan. Sintesis telah dilengkapkan pada 900°C suhu penyepuhlingapan. Untuk AS, kompaun mullite telah dijumpa dan disahkan dengan analisis XRD pada 1300°C dan 1400°C suhu penyepuhlingapan. Dari pemerhatian, evolusi pada ST

bermula membentuk bijiran dari gumpalan serbuk. Dengan peningkatan suhu penyepuhlingdapan, bijiran terus mengembang melalui proses membentuk leher. Proses evolusi hampir menamat apabila sempadan bijiran meresap antara satu sama lain bagi membentuk bijiran yang lebih besar. Dengan perbandingan dua siri sampel ST yang disinter pada 1400°C, purata saiz bijiran oleh sampel dengan permulaan saiz zarah yang lebih besar adalah 0.640 μm manakala yang satu lagi adalah 0.496 μm . ST45 (disaring dengan ayak ujian 45 μm) mengalami pembentukan bijiran yang pesat pada peringkat akhir penyepuhlingdapan manakala pembentukan bijiran ST20 (disaring dengan ayak ujian 45 μm) lebih perlahan. Bagi AS, bijiran bentuk jalur telah diperhatikan dalam sampel yang disinter pada 1400°C. Sample ST dengan permulaan saiz zarah yang lebih besar akan membentuk bijiran yang lagi besar.

Pada ukuran frekuensi rendah, pemalar dielektrik bergantung kepada frekuensi. Saiz bijiran akan menukarkan pemalar dielektrik ST yang bergantung pada suhu pengukuran. Tangen kehilangan, $\tan \delta$ bergantung pada suhu pengukuran. Puncak kehilangan adalah amat berkaitan dengan frekuensi dan suhu pengukuran. Gumpalan serbuk akan menggalakan pengaliran arus ulang alik pada suhu pengukuran yang tinggi dan menurunkan nilai pemalar dielektrik. Nilai pemalar dielektrik ST20 adalah lebih besar dari ST45 kerana kesan pengutupan antara muka yang lebih kuat belaku dalam ST20. ST20 mengandungi saiz bijiran yang kecil yang dapat meningkatkan kesan permukaan. Akibat pembentukan bijiran yang pesat dalam ST45 telah mengurangkan prestasi sifat dielektriknya. Sifat dielektrik ST bergantung kepada saiz bijiran. Kadar pembentukan bijiran yang perlahan adalah amat penting untuk menggalakan saiz bijiran yang homogen dan taburan bijiran semasa evolusi mikrostruktur ST. Saiz zarah yang lebih kecil dan homogen merupakan faktor-faktor amat penting bagi membentuk seramik ST yang bermutu tinggi dengan sifat dielektrik yang bagus. Bagi pengukuran pada frekuensi gelombangmikro, apabila frekuensi telah melebihi 10^7 Hz, nilai pemalar dielektrik akan tetap sepanjang peningkatan frekuensi. Sifat dielektirk ST bergantung kepada saiz bijiran. ST dengan struktur kristal yang lengkap akan menunjuk nilai pamalar dielektrik yang lebih besar.

ACKNOWLEDGEMENTS

I would firstly like to express my deepest gratitude to my supervisor, Assoc. Prof. Dr. Jumiah Hassan for her unwavering encouragement, guidance which enabled me to complete this study. I appreciate this great opportunity and platform that enhanced me towards better understanding of a research in related to materials with microstructure evolutions and dielectric properties.

Secondly, it is my pleasure to learn from my co-supervisors: Assoc. Prof. Dr. Mansor Hashim and Assoc. Prof. Dr. Wan Daud Wan Yusoff. They had been giving me constant advices and supports in order to improve the quality of this research.

I would like to extend my appreciations to my lab colleagues, Wong Swee Yin, Alex See, Tan Foo Khoo, Wong Yick Jeng and others for their help towards the success of this research. Also, I would like to acknowledge the technical staffs of XRD Unit and Electron Microscopy Unit for their kind assistance.

Last but not the least, I offer my regards and blessings to all of those who supported me in any respect during the completion of the project especially my family and friends who have been showering me with their ever-lasting support, encouragement, patience and concern are the main key for me to complete my research successfully.

I certify that a Thesis Examination Committee has met on 7 May 2015 to conduct the final examination of Leow Chun Yan on his thesis entitled “Influence of Microstructure Evolution on Dielectric Properties of Strontium Titanate and Alumina Silicate” in accordance with the Universities and University Colleges Act 1971 and the Constitution of the Universiti Putra Malaysia [P.U.(A) 106] 15 March 1998. The Committee recommends that the student be awarded the Master of Science.

Members of the Thesis Examination Committee were as follows:

Zaidan bin Abdul Wahab, PhD

Associate Professor
Faculty of Science
Universiti Putra Malaysia
(Chairman)

Mohd Maarof bin Abd Moxsin, PhD

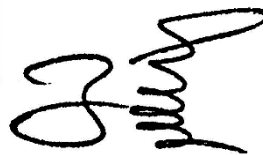
Professor
Faculty of Science
Universiti Putra Malaysia
(Internal Examiner)

Chen Soo Kien, PhD

Associate Professor
Faculty of Science
Universiti Putra Malaysia
(Internal Examiner)

Rosli Hussin, PhD

Professor
Universiti Teknologi Malaysia
Malaysia
(External Examiner)



ZULKARNAIN ZAINAL, PhD

Professor and Deputy Dean
School of Graduate Studies
Universiti Putra Malaysia

Date: 7 July 2015

This thesis was submitted to the Senate of Universiti Putra Malaysia and has been accepted as fulfilment of the requirement for the degree of Master of Science. The members of the Supervisory Committee were as follows:

Jumiah binti Hassan, PhD

Associate Professor
Faculty of Science
Universiti Putra Malaysia
(Chairman)

Mansor bin Hashim, PhD

Associate Professor
Faculty of Science
Universiti Putra Malaysia
(Member)

Wan Daud Wan Yusoff, PhD

Associate Professor
Faculty of Science
Universiti Putra Malaysia
(Member)

BUJANG BIN KIM HUAT, PhD

Professor and Deputy Dean
School of Graduate Studies
Universiti Putra Malaysia

Date: 7 July 2015

Declaration by graduate student

I hereby confirm that:

- this thesis is my original work;
- quotations, illustrations and citations have been duly referenced;
- this thesis has not been submitted previously or concurrently for any other degree at any other institutions;
- intellectual property from the thesis and copyright of thesis are fully-owned by Universiti Putra Malaysia, as according to the Universiti Putra Malaysia (Research) Rules 2012;
- written permission must be obtained from supervisor and the office of Deputy Vice-Chancellor (Research and Innovation) before thesis is published (in the form of written, printed or in electronic form) including books, journals, modules, proceedings, popular writings, seminar papers, manuscripts, posters, reports, lecture notes, learning modules or any other materials as stated in the Universiti Putra Malaysia (Research) Rules 2012;
- there is no plagiarism or data falsification/fabrication in the thesis, and scholarly integrity is upheld as according to the Universiti Putra Malaysia (Graduate Studies) Rules 2003 (Revision 2012-2013) and the Universiti Putra Malaysia (Research) Rules 2012. The thesis has undergone plagiarism detection software.

Signature: _____ Date: _____

Name and Matric No.: _____

Declaration by Members of Supervisory Committee

This is to confirm that:

- the research conducted and the writing of this thesis was under our supervision;
- supervision responsibilities as stated in the Universiti Putra Malaysia (Graduate Studies) Rules 2003 (Revision 2012-2013) are adhered to.

Signature: _____
Name of Chairman of
Supervisory
Committee: _____

Signature: _____
Name of Member of
Supervisory
Committee: _____

TABLE OF CONTENTS

	Page
ABSTRACT	i
ABSTRAK	iii
ACKNOWLEDGEMENTS	v
APPROVAL	vi
DECLARATION	viii
LIST OF TABLES	xii
LIST OF FIGURES	xiii
LIST OF ABBREVIATIONS	xvii
CHAPTER	
1 INTRODUCTION	1
1.1 Ceramics	1
1.2 Strontium Titanate, SrTiO ₃	2
1.3 Alumina Silicate, Al ₂ SiO ₅	3
1.4 Background and importance of studies	5
1.5 Objectives	6
1.6 Limitations	6
2 LITERATURE REVIEW	7
2.1 Introduction	7
2.2 Reviews on Strontium Titanate	7
2.3 Reviews on Alumina Silicate	9
3 THEORY	11
3.1 Theory of sintering mechanism and process	11
3.2 Evolution mechanism on ceramic microstructure	12
3.3 Theory of dielectric properties	14
3.3.1 Capacitor and capacitance	14
3.3.2 Complex permittivity	16
3.4 Dielectric polarization	18
3.4.1 Electronic polarization	19
3.4.2 Ionic polarization	19
3.4.3 Orientation polarization	19
3.4.4 Interfacial polarization	19
3.4.5 Frequency dependence	20
4 METHODOLOGY	22
4.1 General	22
4.2 Sample preparation procedures	23
4.2.1 Weighing	25
4.2.2 Ball milled mixing	25
4.2.3 Pre-sintering	25
4.2.4 Grinding	26
4.2.5 Sieving	26

4.2.6	Sample molding	26
4.2.7	Final sintering	26
4.3	Experimental measurement	27
4.3.1	X-Ray Diffraction (XRD) analysis	27
4.3.2	Microstructure analysis	27
4.3.3	Dielectric measurements	28
4.3.3.1	Low frequency measurement	28
4.3.3.2	Microwave frequency measurement	29
5	RESULTS AND DISCUSSION	30
5.1	General	30
5.2	X-Ray Diffraction (XRD) analysis	30
5.2.1	Strontium Titanate (SrTiO ₃)	30
5.2.2	Alumina Silicate (Al ₂ SiO ₅)	35
5.3	Microscopic morphology and grain size analysis.	37
5.3.1	ST45 sample FESEM micrograph analysis	37
5.3.2	ST20 sample FESEM micrograph analysis	42
5.3.3	AS sample FESEM micrograph analysis	47
5.4	Dielectric properties at low frequency	52
5.4.1	Dielectric constant of ST45 at low frequency	52
5.4.2	Loss tangent of ST45 at low frequency	53
5.4.3	Dielectric constant of ST20 at low frequency	57
5.4.4	Loss tangent of ST20 at low frequency	58
5.4.5	Dielectric constant of AS at low frequency	63
5.4.6	Loss tangent of AS at low frequency	64
5.5	Dielectric properties at microwave frequency	68
5.5.1	Dielectric constant of ST45 and ST20 at microwave frequency	68
5.5.2	Loss tangent of ST45 and ST20 at microwave frequency	68
5.5.3	Dielectric constant of AS at microwave frequency	71
5.5.4	Loss tangent of AS at microwave frequency	71
6	CONCLUSION	73
6.1	X-Ray Diffraction (XRD) analysis	73
6.2	Microstructure analysis	73
6.3	Dielectric properties analysis	73
6.4	Further study	74
	BIBLIOGRAPHY	75
	BIODATA OF STUDENT	82
	LIST OF PUBLICATIONS	83

LIST OF TABLES

Table		Page
3.1	Sintering process effects	12
4.1	Starting materials identities and contents	23
5.3.1	Average grain size of ST45 samples at various sintering temperatures	38
5.3.2	Average grain size of ST20 samples at various sintering temperatures	44
5.3.3	Average grain size of Alumina Silicate samples at various sintering temperatures	48



LIST OF FIGURES

Figure		Page
1.1	Cubic perovskite structure of ST	3
1.2	Crystal structure of sillimanite in projection down c axis and a axis (Simple model of sillimanite and mullite are alike)	4
3.1	Sintering stages	13
3.2	Parallel plate capacitor connected to a closed circuit	14
3.3	Parallel plate capacitor in vacuum and dielectric material inserted between the plates.	16
3.4	Relationship between applied AC voltage and the resultant current	18
3.5	Charge distribution built in the dielectric material	18
3.6	Types of polarization mechanism	20
3.7	Types of polarization mechanism dependent of frequency	21
4.1	Summary of samples preparation	24
5.2.1	XRD patterns for ST45 samples at sintering temperatures 500°C to 1400°C	32
5.2.2	XRD patterns for ST20 samples at sintering temperatures 500°C to 1400°C	34
5.2.3	XRD patterns for AS samples at sintering temperatures 500°C to 1400°C	36
5.3.1	(a) FESEM micrograph with magnification of 60,000 x and (b) Grain size distribution of ST45 sample sintered at 500°C	38
5.3.2	(a) FESEM micrograph with magnification of 60,000 x and (b) Grain size distribution of ST45 sample sintered at 600°C	39
5.3.3	(a) FESEM micrograph with magnification of 60,000 x and (b) Grain size distribution of ST45 sample sintered at 700°C	39
5.3.4	(a) FESEM micrograph with magnification of 60,000 x and (b) Grain size distribution of ST45 sample sintered at 800°C	39
5.3.5	(a) FESEM micrograph with magnification of 60,000 x and (b) Grain size distribution of ST45 sample sintered at 900°C	40
5.3.6	(a) FESEM micrograph with magnification of 60,000 x and (b) Grain size distribution of ST45 sample sintered at 1000°C	40
5.3.7	(a) FESEM micrograph with magnification of 60,000 x and (b) Grain size distribution of ST45 sample sintered at 1100°C	40
5.3.8	(a) FESEM micrograph with magnification of 60,000 x and (b) Grain size distribution of ST45 sample sintered at 1200°C	41
5.3.9	(a) FESEM micrograph with magnification of 60,000 x and (b) Grain size distribution of ST45 sample sintered at 1300°C	41
5.3.10	(a) FESEM micrograph with magnification of 60,000 x and (b) Grain size distribution of ST45 sample sintered at 1400°C	41
5.3.11	(a) FESEM micrograph with magnification of 60,000 x and (b) Grain size distribution of ST20 sample sintered at 500°C	44
5.3.12	(a) FESEM micrograph with magnification of 60,000 x and (b) Grain size distribution of ST20 sample sintered at 600°C	44
5.3.13	(a) FESEM micrograph with magnification of 60,000 x and (b) Grain size distribution of ST20 sample sintered at 700°C	45

5.3.14	(a) FESEM micrograph with magnification of 60,000 x and (b) Grain size distribution of ST20 sample sintered at 800°C	45
5.3.15	(a) FESEM micrograph with magnification of 60,000 x and (b) Grain size distribution of ST20 sample sintered at 900°C	45
5.3.16	(a) FESEM micrograph with magnification of 60,000 x and (b) Grain size distribution of ST20 sample sintered at 1000°C	46
5.3.17	(a) FESEM micrograph with magnification of 60,000 x and (b) Grain size distribution of ST20 sample sintered at 1100°C	46
5.3.18	(a) FESEM micrograph with magnification of 60,000 x and (b) Grain size distribution of ST20 sample sintered at 1200°C	46
5.3.19	(a) FESEM micrograph with magnification of 60,000 x and (b) Grain size distribution of ST20 sample sintered at 1300°C	47
5.3.20	(a) FESEM micrograph with magnification of 60,000 x and (b) Grain size distribution of ST20 sample sintered at 1400°C	47
5.3.21	(a) FESEM micrograph with magnification of 60,000 x and (b) Grain size distribution of AS sample sintered at 500°C	49
5.3.22	(a) FESEM micrograph with magnification of 60,000 x and (b) Grain size distribution of AS sample sintered at 600°C	49
5.3.23	(a) FESEM micrograph with magnification of 60,000 x and (b) Grain size distribution of AS sample sintered at 700°C	49
5.3.24	(a) FESEM micrograph with magnification of 60,000 x and (b) Grain size distribution of AS sample sintered at 800°C	50
5.3.25	(a) FESEM micrograph with magnification of 60,000 x and (b) Grain size distribution of AS sample sintered at 900°C	50
5.3.26	(a) FESEM micrograph with magnification of 60,000 x and (b) Grain size distribution of AS sample sintered at 1000°C	50
5.3.27	(a) FESEM micrograph with magnification of 60,000 x and (b) Grain size distribution of AS sample sintered at 1100°C	51
5.3.28	(a) FESEM micrograph with magnification of 60,000 x and (b) Grain size distribution of AS sample sintered at 1200°C	51
5.3.29	(a) FESEM micrograph with magnification of 60,000 x and (b) Grain size distribution of AS sample sintered at 1300°C	51
5.3.30	(a) FESEM micrograph with magnification of 60,000 x and (b) Grain size distribution of AS sample sintered at 1400°C	52
5.4.1	Frequency dependence of (a) ϵ_r' and (b) $\tan \delta$ of ST45 sample sintered at 500°C at various measuring temperatures.	54
5.4.2	Frequency dependence of (a) ϵ_r' and (b) $\tan \delta$ of ST45 sample sintered at 600°C at various measuring temperatures	54
5.4.3	Frequency dependence of (a) ϵ_r' and (b) $\tan \delta$ of ST45 sample sintered at 700°C at various measuring temperatures	55
5.4.4	Frequency dependence of (a) ϵ_r' and (b) $\tan \delta$ of ST45 sample sintered at 800°C at various measuring temperatures	55
5.4.5	Frequency dependence of (a) ϵ_r' and (b) $\tan \delta$ of ST45 sample sintered at 900°C at various measuring temperatures	55
5.4.6	Frequency dependence of (a) ϵ_r' and (b) $\tan \delta$ of ST45 sample sintered at 1000°C at various measuring temperatures	56
5.4.7	Frequency dependence of (a) ϵ_r' and (b) $\tan \delta$ of ST45 sample sintered at 1100°C at various measuring temperatures	56
5.4.8	Frequency dependence of (a) ϵ_r' and (b) $\tan \delta$ of ST45 sample sintered at 1200°C at various measuring temperatures	56

5.4.9	Frequency dependence of (a) ϵ_r' and (b) $\tan \delta$ of ST45 sample sintered at 1300°C at various measuring temperatures	57
5.4.10	Frequency dependence of (a) ϵ_r' and (b) $\tan \delta$ of ST45 sample sintered at 1400°C at various measuring temperatures	57
5.4.11	Frequency dependence of (a) ϵ_r' and (b) $\tan \delta$ of ST20 sample sintered at 500°C at various measuring temperatures.	60
5.4.12	Frequency dependence of (a) ϵ_r' and (b) $\tan \delta$ of ST20 sample sintered at 600°C at various measuring temperatures.	60
5.4.13	Frequency dependence of (a) ϵ_r' and (b) $\tan \delta$ of ST20 sample sintered at 700°C at various measuring temperatures.	60
5.4.14	Frequency dependence of (a) ϵ_r' and (b) $\tan \delta$ of ST20 sample sintered at 800°C at various measuring temperatures.	61
5.4.15	Frequency dependence of (a) ϵ_r' and (b) $\tan \delta$ of ST20 sample sintered at 900°C at various measuring temperatures.	61
5.4.16	Frequency dependence of (a) ϵ_r' and (b) $\tan \delta$ of ST20 sample sintered at 1000°C at various measuring temperatures.	61
5.4.17	Frequency dependence of (a) ϵ_r' and (b) $\tan \delta$ of ST20 sample sintered at 1100°C at various measuring temperatures.	62
5.4.18	Frequency dependence of (a) ϵ_r' and (b) $\tan \delta$ of ST20 sample sintered at 1200°C at various measuring temperatures.	62
5.4.19	Frequency dependence of (a) ϵ_r' and (b) $\tan \delta$ of ST20 sample sintered at 1300°C at various measuring temperatures.	62
5.4.20	Frequency dependence of (a) ϵ_r' and (b) $\tan \delta$ of ST20 sample sintered at 1400°C at various measuring temperatures.	64
5.4.21	Figure 5.4.21 Frequency dependence of (a) ϵ_r' and (b) $\tan \delta$ of AS sample sintered at 500°C at various measuring temperatures.	64
5.4.22	Figure 5.4.21 Frequency dependence of (a) ϵ_r' and (b) $\tan \delta$ of AS sample sintered at 600°C at various measuring temperatures.	65
5.4.23	Figure 5.4.21 Frequency dependence of (a) ϵ_r' and (b) $\tan \delta$ of AS sample sintered at 700°C at various measuring temperatures.	65
5.4.24	Figure 5.4.21 Frequency dependence of (a) ϵ_r' and (b) $\tan \delta$ of AS sample sintered at 800°C at various measuring temperatures.	65
5.4.25	Figure 5.4.21 Frequency dependence of (a) ϵ_r' and (b) $\tan \delta$ of AS sample sintered at 900°C at various measuring temperatures.	66
5.4.26	Figure 5.4.21 Frequency dependence of (a) ϵ_r' and (b) $\tan \delta$ of AS sample sintered at 1000°C at various measuring temperatures.	66
5.4.27	Figure 5.4.21 Frequency dependence of (a) ϵ_r' and (b) $\tan \delta$ of AS sample sintered at 1100°C at various measuring temperatures.	66
5.4.28	Figure 5.4.21 Frequency dependence of (a) ϵ_r' and (b) $\tan \delta$ of AS sample sintered at 1200°C at various measuring temperatures.	67
5.4.29	Figure 5.4.21 Frequency dependence of (a) ϵ_r' and (b) $\tan \delta$ of AS sample sintered at 1300°C at various measuring temperatures.	67
5.4.30	Figure 5.4.21 Frequency dependence of (a) ϵ_r' and (b) $\tan \delta$ of AS sample sintered at 1400°C at various measuring temperatures.	67
5.5.1	Frequency dependence of dielectric constant, ϵ_r' of ST45 sample sintered at various temperatures measured at room temperature	69
5.5.2	Frequency dependence of dielectric constant, ϵ_r' of ST20 sample sintered at various temperatures measured at room temperature	69
5.5.3	Frequency dependence of loss tangent, $\tan \delta$ of ST45 sample sintered at various temperatures measured at room temperature	70

5.5.4	Frequency dependence of loss tangent, $\tan \delta$ of ST20 sample sintered at various temperatures measured at room temperature	70
5.5.5	Frequency dependence of dielectric constant, ϵ_r' of AS sample sintered at various temperatures measured at room temperature	71
5.5.6	Frequency dependence of loss tangent, $\tan \delta$ of AS sample sintered at various temperatures measured at room temperature	72



LIST OF ABBREVIATIONS

C	Capacitance
G	Conductance
f	Frequency
E	Electric Field
σ	Magnitude of Surface Charge Density
Q	Magnitude of Total Charge
V	Potential Difference
A	Area of Each Plate / Area of sample
d	Separation between the plates
C_{vac}	Capacitance of Parallel Plates in Vacuum
ϵ_0	Permittivity of Free Space
ϵ^*	Complex Permittivity
ϵ_r^*	Relative Complex Permittivity
j	Imaginary Operator with $(-1)^{1/2}$
ϵ_r'	Relative Dielectric Constant
ϵ_r''	Relative Dielectric Loss Factor
δ	Loss angle
$\tan \delta$	Dielectric Loss Tangent
n	Order of the Diffracted Beam
λ	Wavelength of the Incident X-Ray Beam
hkl	Lattice Plane
d_{hkl}	Spacing Between atomic planes
θ_{hkl}	Angle of the Incident X-Ray
$^\circ$	Degree
$^\circ\text{C}$	Degree Celsius
Hz	Hertz

Short Form	Description
Al	Aluminum
Ba	Barium
Ca	Calcium
O	Oxygen
Sr	Strontium
Ta	Tantalum
Ti	Titanaium
Zr	Zirconium
Al ₂ SiO ₅	Alumina Silicate
Al ₂ O ₃	Aluminum Oxide
SiO ₂	Silicon Oxide
SrTiO ₃	Strontium Titanate
SrCO ₃	Strontium Carbonate
SrO ₂	Strontium Peroxide
Sr(NO ₃) ₂	Strontium Nitrate
BaTiO ₃	Barium Titanate
N ₂	Nitrogen Gas
Fe ₂ O ₃	Iron Oxide
ac	Alternating Current
AS	Alumina Silicate
DRAM	Dynamic Random Access Memories
FESEM	Field Emission Scanning Electron Microscope
GBLC	Grain Boundary Layer Capacitor
ICDD	International Centre for Diffraction Data
SEM	Scanning Electron Microscope
T _c	Curie temperature
XRD	X-ray Diffraction
YBCO	Y-Ba-Cu-O Superconductor

CHAPTER 1

INTRODUCTION

1.1 Ceramics

Typical ceramics may be defined as inorganic non-metallic material, which occur in crystalline structure, partial crystalline structure or amorphous form. Ceramics offer many advantages compared to other materials. Comparing with other materials, ceramics are far more chemically inert and durable. Besides, they also demonstrate excellent strength and hardness properties. They are harder and stiffer than steel. Ceramics do not deform easily at ordinary temperatures (Tilley, 2004). Due to its outstanding chemical inert properties, ceramics are more corrosion resistant than metals or polymers. Although with all kinds of pros as mentioned, ceramics does have some cons in nature. Generally, ceramics are brittle and easy to fracture under impact. However, even ceramics are readily fractured when stretched; they are much stronger when compressed.

Ceramic is an important material throughout the history of humankind. Even until today and in the future, ceramic is still has it crucial roles to play in modern technology. People may underestimate the potential applications of ceramics because they believe ceramics are all about pottery and tiles. In fact, besides this kind of traditional use, ceramic also possess outstanding properties that are suitable for modern technology especially in electronic industries. The evolution from pottery to electronic components has broadened the term 'ceramic' (Moulson et.al., 1990). Ceramic materials display a wide range of properties that facilitate their use in many different potential areas. Advanced ceramic has different functions in different fields. Among the fields are electrical, magnetic optical, biomedical and many others. In electrical field, applications of ceramic are broad. Ceramic BaTiO_3 and SrTiO_3 are representative in capacitors and microwave dielectrics. For superconductors is $\text{YBa}_2\text{Cu}_3\text{O}_{7-x}$ (YBCO). Ceramics are also used as piezoelectric material, electrical insulator and solid-oxide fuel cell that are under electrical field (Askeland et. al., 2003).

Ferrite-type and garnet-type ceramics are representative in magnetic field. Magnets, inductors (choke), circulators and isolators mostly are made from ferrite and garnet type ceramics. They are the core in transformers and microwave technology (Askeland et. al., 2003; Moulson et.al., 1990). SiO_2 and Al_2O_3 based ceramics mostly function in optical field. Normally they are made into glasses and as based material in lasers. Under biomedical field, ceramics serve as implants such as dental materials. Finally, yet importantly is the contribution of ceramic in construction and domestic application, for examples: concretes, tiles, sanitary wares and kitchenwares. With all the functions and application of ceramic, it is like a great gift from the creator of the world. We should not take it for granted and must use it wisely.

1.2 Strontium Titanate, SrTiO₃

Strontium Titanate (ST) or Tausonite named to honour Lev Vladimirovich Tauson (1917–1989), a Russian geochemist petrologist. ST with chemical formula SrTiO₃ is an oxide of Strontium and Titanium. In nature, ST mineral is extremely rare and usually it occurred in a form of very tiny crystal. Almost all ST use in application is synthetically prepared by raw materials rather than from ore extractions.

ST may occur in brown, red-brown, grey and dark grey colour. Its Mohs Hardness value is around 6.0 – 6.5 while for diamond is 10. As a typical ceramic material, ST is brittle and may show conchoidal fracture when it breaks. Conchoidal fracture is the way it breaks that do not follow any natural planes of separation. Theoretical density of ST is 4.81 g cm⁻³. Its melting point is 2080 °C. At room temperature, ST has dielectric constant around 330 and dielectric loss of the order of 10⁻³ (Jacob et al., 2011).

Application of ST is mostly found in electronic industries. ST has no phase transformation above the ferroelectric - paraelectric transition temperature, T_c. It possessed excellent stable dielectric properties and stable temperature characteristics (Zhao et al., 2004). With these excellent properties, ST is suitable for use in grain boundary layer capacitor (GBLC) and as thin film in dynamic random access memories (DRAMs) (Roy et al., 2005). ST may also become a good microwave tunable device in situations of dependence in high dc electric field (Amaral et al., 2009). Besides, ST exhibits nonlinear current–voltage (I–V) characteristic that is suitable to be used as varistor (Li et al., 2006). Furthermore, ST is also important in other applications such as oxygen gas sensor, diamond stimulant and as substrate for the hetero-epitaxial growth of high T_c-superconductors (Wang et al., 2008; Roy et al., 2005). Since ST has the outstanding characteristic in its applications, until today it is still a worthy material to research and study.

Seeing that ST has such excellent characteristic in a wide range of applications, it aroused many researchers interest and attention, to study what is the reason that made ST such an outstanding material. From material scientist point of view, macroscopic properties of a material may always be affected by its structure at atomic or molecular scales. ST appeared in perovskite structure form. Perovskite is a family name of ABO₃ compound group where A and B differ in size. Normally, A is a large radius cation of coordinate 12 (example: Ba, Sr, Ca, Pb) which occupies the empty sites between oxygen (O) octahedral. B will be a smaller radius cation of coordinate 6 (example: Ti, Zr, Nb, Ta) (Bunget et. al., 1984).

At room temperature, ST is in cubic perovskite structure with space group *Pm3m* (Shkabko et al., 2009). In the structure, Oxygen (O) ions formed octahedron structure lies in the body- and face-centred cubic structure formed by A-Strontium (Sr) and B-Titanium (Ti) ions (Figure 1.1). SrTiO₃ compound with this structure possessed paraelectric characteristic. Either the distortions of the oxygen octahedra gathering or decentration distortion of ion B in oxygen octahedra may dramatically change the characteristic of the materials. For example, Barium Titanate (BaTiO₃) has distorted B

ions (Ti) at room temperature that makes it become tetragonal structure. Displacement of B ions (Ti) with O ions changed the interatomic bonding forces that increase the covalency of B-O bond. This interesting phenomenon has made Barium Titanate a famous ferroelectric material (Bunget et., al. 1984).

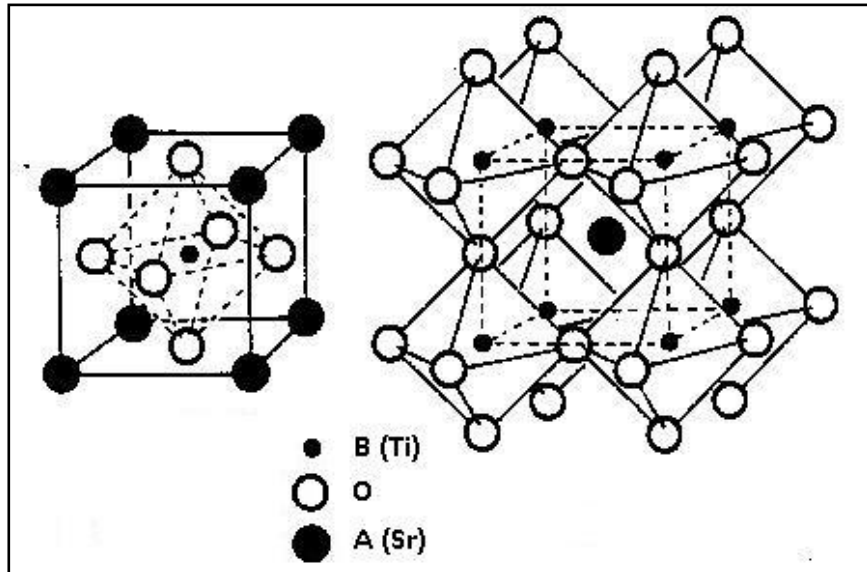


Figure 1.1 Cubic Perovskite Structure of ST (Xu,1991)

1.3 Alumina Silicate, Al_2SiO_5

Alumina Silicate or Aluminum Silicate (AS) mainly is formed by mixture of Aluminium (Al), Silica (Si) and Oxygen (O). AS exist in several crystal structure forms by nature or depending on the synthesis condition. During synthesis, under different conditions of pressure and temperature, different crystalline forms and phase may occur. They could be kyanite, andalusite, sillimanite, mullite, kaolinite (combination of AS with water) and others. Kyanite, sillimanite and andalusite are the polymorphs occurring in AS minerals (Whitney, 2002). Kyanite forms in a lower temperature/higher pressure environment, andalusite forms in a lower temperature/lower pressure environment, while sillimanite forms in a higher temperature/higher pressure environment. For mullite, the molecular ratio is $3\text{Al}_2\text{O}_3 \cdot 2\text{SiO}_2$. Mullite rarely occur as a mineral in nature. It is commonly formed by synthesis. Chemical formula for all of these crystalline forms and phase is Al_2SiO_5 . Although they have the same chemical formula, they do exhibit some common and unique physical and chemical properties.

Most of AS ceramics have common properties of high melting point (Baker et. al., 2006), good thermal and chemical stability (Naga et. al., 1992). With excellent high temperature properties, AS products normally would serve as refractory material, fire

protection, metal melting and engineering applications. (Laskowski et. al., 1994; Baker et. al., 2006)

In this work, mullite is the material to be studied. Mullite a promising material that widely being use in traditional and advanced ceramics. It is outstanding with electrical, thermal and mechanical properties. The advantageous properties of mullite include high melting point, high temperature strength, excellent creep and chemical resistance, strong heat and electrical insulation and finally yet importantly are its low thermal expansion coefficient (Ebadzadeh et. al., 2009; Sainz et. al., 2000). Low loss in dielectric, good thermal and chemical stability allow mullite to perform as advanced ceramic for use in electronic packaging materials (thermal and electronic insulation purpose). Besides, mullite fibers are used for coating and even as a matrix to enhance composite materials. As a traditional ceramics, mullite is use as white wares, structural materials and refractory materials (Chen and Lan, 2000; Schneider et. al., 2005).

Mullite is orthorhombic - dipyramidal class with space group $Cmmm$. The average structure of mullite can be derived from the closely related but structurally simpler sillimanite. In sillimanite, like in other mullite type structures, edge-connected AlO_6 octahedral chains run parallel to the crystallographic c-axis in Figure 1.2. In sillimanite these octahedral chains are cross-linked by double chains with alternating AlO_4 and SiO_4 tetrahedra (Figure 1.2). Mullite can be derived from sillimanite by a coupled substitution, according to $2Si^{4+} + O^{2-} \rightarrow 2Al^{3+} + X$, $X =$ oxygen vacancy. This reaction involves removal of oxygen atoms from the structure leading to oxygen vacancies and to a rearrangement and disordering of tetrahedral cations (Schneider et. al., 2008; Schneider et. al., 2005). Understanding the structure of mullite is an important key to study its excellent properties.

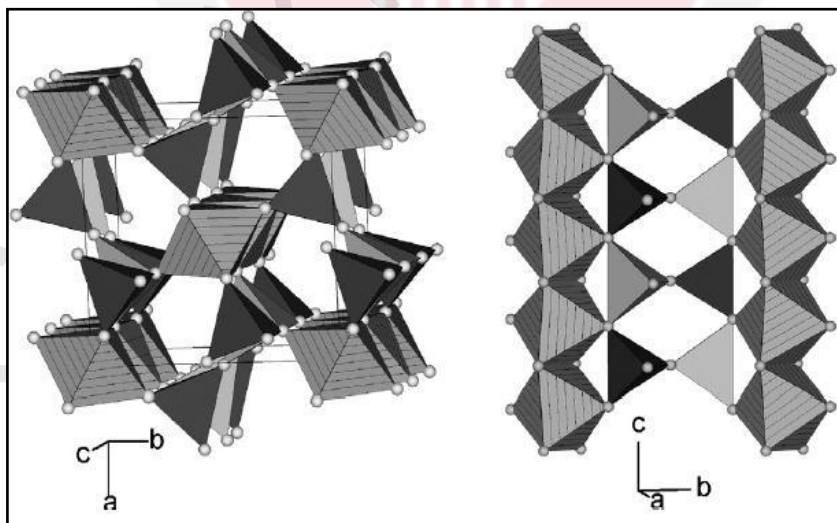


Figure 1.2: Crystal Structure of Sillimanite in projection down c axis and a axis (Simple model of Sillimanite and Mullite are alike) (Schneider et. al., 2008)

1.4 Background and importance of studies

Recent reports about Strontium Titanate (ST) and Alumina Silicate (AS) rarely studied on their dielectric properties across wide range of sintering temperatures. There are very few reviews made on a detailed study relating them from initial stage to final stage of sintering along with the microstructure and the dielectric properties are evolving towards their final form and values. Most of the studies often focus on the after formation of its crystal structure phase and microstructure changes towards the dielectric properties. In fact, these studies are lacks of information link with the early synthesis process.

The present research proposal intends to deal with these little understood aspects. In this study, ST and AS microstructure evolution were analyzed in parallel with their dielectric properties along with wide range sintering temperatures from 500°C to 1400°C. Microstructure changes in a ceramic material will always influence its application properties in parallel. As for sintering process, often, average grain size of a sample is one of the important key to unlock the information about microstructure evolution. In order to have a glance on microstructure evolution, grain size analysis is necessary to be studied.

Besides grain size analysis, X-Ray Diffraction (XRD) analysis needed to be carried out in order to study and confirmed the formation of crystal structure phase of ST and AS. Across wide range of sintering process, crystal structure formation needed to be studied along with the microstructure evolution to get a clearer picture on how the sintering temperature might affects the process. XRD analysis might provide more information to support the microstructure analysis.

Materials microstructure formation also is dependent on the parameters of its starting materials. Particle size of a starting material is one of the important parameter to influence the microstructure formation in most of the ceramic materials. Conventional solid-state reaction methods are the simplest and most widely used method to synthesize ceramics. In order to study the particular effects of starting materials particle size for ST, two different sieving size were set during solid-state reaction method was carried out. Different particle sizes of starting material will have yield different outcome for the microstructure morphology and they might influences the dielectric properties as well.

Dielectric measurements are performed at frequencies from 40 Hz to 1.8 GHz. Within this frequency range, it is the optimum condition to analyse the dielectric properties of the samples for application. Strontium Titanate and Alumina Silicate are well known for their stable dielectric properties performance at temperature above 100°C. Various measuring temperature were set parallel during the dielectric measurement is being carried out. From this study, the optimization process for microstructure phase formation may lead to optimize its dielectric properties. Analysis of the data obtained can be extended to other alumina and titanate based materials for the development of multilayer capacitors.

1.5 Objectives

Strontium Titanate and Alumina Silicate samples are synthesized at sintering temperature range from 500°C - 1400°C. Across this sintering temperature:

1. Samples preparation were set with two different particle sizes using conventional solid-state reaction method. This setting is made in order to investigate the fundamental core that influence the microstructure formation.
2. Crystal structure formation of samples are analyzed by XRD analysis and average grain size of samples are determined from the Scanning Electron Microscopy (SEM) micrograph. Both these methods will monitored the crystal structure formation and microstructure evolution along with increasing sintering temperature.
3. Dielectric properties of samples are studied from 40 Hz to 1.8 GHz frequency range with different measuring temperature. Relationship between the dielectric properties and microstructure of the samples were studied in parallel in order to have a better and deeper understanding on this mutual dependent parameters.

1.6 Limitations

1. All samples are only prepared by conventional solid state reaction method and the particle sizes are limited at micron size range.
2. Sintering temperature of AS samples are limited only to 1400°C due to furnace limitation (no furnace higher than 1400°C was available).

BIBLIOGRAPHY

- Amaral, L., Senos, A. M.R., Vilarinho, P.M. (2009). Sintering kinetic studies in nonstoichiometric strontium titanate ceramics. *Materials Research Bulletin* 44: 263–270.
- Askeland, D.R., Phule, P.P. (2003). *The Science and Engineering of Materials (Fourth Edition)*. Brooks/Cole – Thomson Learning 511 Forest Lodge Road Pacific Grove, CA 93950 USA.
- Baker, T.J., Zimba, J., Akpan, E.T., Bashir, I., Watola, C.T., Soboyejo, W.O. (2006). Viscoelastic toughening of aluminosilicate refractory ceramics. *Acta Materialia* 54: 2665–2675.
- Barde, R.V., Nemade, K.R., Waghuley, S.A. (2014). AC conductivity and dielectric relaxation in V_2O_5 – P_2O_5 – B_2O_3 glasses. *Journal of Asian Ceramic Societies*
- Barsoukov, E., Macdonald, J.R. (2005). *Impedance Spectroscopy: Theory, Experiment, and Applications, 2nd Edition*. John Wiley and Sons, Inc.
- Berbenni, V., Marini, A., Bruni, G. (2001). Effect of mechanical activation on the preparation of $SrTiO_3$ and Sr_2TiO_4 ceramics from the solid state system $SrCO_3$ – TiO_2 . *Journal of Alloys and Compounds* 329: 230–238.
- Bötcher, C.J.F., and Bordewijk, P. (1978) *Dielectrics in Time Dependent Fields, Second Edition*. Elsevier Scientific Publishing Company, Amsterdam.
- Bowen, D.K., Hall, C.R. (1975). *Microscopy of materials*. The Macmillan Press Ltd.
- Brown, W.D., Hess, D., Desai, V., Deen, M.J. (2006) Dielectric science and technology. *The Electrochemical Society Interface* 15: 28-31
- Bunget, I., Popescu, M., (1984). *Physics of Solid Dielectrics*. Elsevier Science Publishers, The Netherlands.
- Chenari, H.M., Golzan, M.M., Sedghi, H., Hassanzadeh, A., Talebian, M. (2011). Frequency dependence of dielectric properties and electrical conductivity of Cu/nano-SnO₂ thick film/Cu arrangement. *Current Applied Physics* 11: 1071-1076.
- Chen, C.Y., Lan, G.S., Tuan, W.H. (2000). Microstructural evolution of mullite during the sintering of kaolin powder compacts. *Ceramics International* 26 :715-720.
- Chen, L.F., Ong, C.K., Neo, C.P., Varadan, V.V., Varadan, V.K. (2004). *Microwave electronics: measurement and materials characterization*. John Wiley & Sons, Inc.

- Chen, L., Zhang, S., Wang, L., Xue, D., Yin, S. (2009). Preparation and photocatalytic properties of strontium titanate powders via sol-gel process. *Journal of Crystal Growth*, 311: 746–748.
- Chen, R., and Marathe, N. (n.d.). *Dielectric polarization*. Retrieved January 30, 2015 from http://chemwiki.ucdavis.edu/u_Materials/Optics/Dielectric_Polarization
- Cho, W.W., Kagomiya, I., Kakimoto, K., Hitoshi, O. (2007). Frequency dependence of dielectric properties of metallodielectric SrTiO₃-Pt composites. *Journal of the European Ceramic Society* 27: 2907–2910.
- Daniel, V.V. (1967) *Dielectric Relaxation*. Academic Press, London.
- Deng, Y.F., Zhou., (2008). Z.H. A stable water-soluble molecular precursor for the preparation of stoichiometric strontium titanate. *Inorganic Chemistry Communications*, 11: 1064–1066.
- Ebadzadeh, T., Sarrafi, M.H., Salahi, E. (2009). Microwave-assisted synthesis and sintering of mullite. *Ceramics International* 35: 3175–3179.
- Fröhlich, H. (1958). *Theory of dielectrics, second edition*. Clarendon Press, Oxford.
- Gao, F., Yang, S., Li, J., Qin, M., Zhang, Y., Sun, H. (2015). Fabrication, dielectric, and thermoelectric properties of textured SrTiO₃ ceramics prepared by RTGG method. *Ceramics International* 41: 27–135.
- German, R.M. (1996). *Sintering Theory and Practice*, John Wiley and Sons, Inc.
- Golstein, J.I., Lyman, C.E., Newbury, D.E., Lifshin, E., Echlin, P., Sawyer, L., Joy, D. C., Michael, J. R. (2003). *Scanning electron microscopy and X-ray microanalysis*. Springer Science + Business Media LLC.
- Guo, A., Liu, Rui Xu, J., Xu, H., Wang, C. (2010). Preparation of mullite from desilication-flyash. *Fuel* 89:3630–3636.
- Hanemann, T., Gesswein, H., Schumacher, B. (2011). Dielectric property improvement of polymer-nanosized strontium titanate-composites for applications in microelectronics. *Microsystem Technologies* 17:1529–1535.
- Hong, S.H., Messing, G.L. (1998) Anisotropic grain growth in diphasic gel-derived titania-doped mullite, *Journal of the American Ceramic Society*, 81: 1269–1277.
- Hu, Q.G., Shen, Z.Y., Li, Y.M., Wang, Z.M., Luo, W.Q., Xie, Z.X. (2014). Enhanced energy storage properties of dysprosium doped strontium titanate ceramics. *Ceramics International* 40: 2529–2534.
- Ianculescu, A., u Synthesis, A. B., Voicu, G., (2007). Microstructure and dielectric properties of antimony-doped strontium titanate ceramics. *Journal of the European Ceramic Society* 27: 1123–1127.

- Ishikawa, H., Oohira, K., Nakajima, T., Akiyama, T. (2008). Combustion synthesis of SrTiO₃ using different raw materials. *Journal of Alloys and Compounds* 454: 384–388.
- Jacob, K.T., Rajitha, G. (2011). Thermodynamic Properties of Strontium Titanates: Sr₂TiO₄, Sr₃Ti₂O₇, Sr₄Ti₃O₁₀, and SrTiO₃. *Journal of Chemical Thermodynamics* 43: 51–57.
- Karthickprabhu, S., Hirankumar, G., Maheswaran, A., Daries Bella, R.S., Sanjeeviraja, C., Junichi, K. (Eds.). (2013). Proceedings of the 13th Asian Conference Solid State Ionics: Ionics for Sustainable World: *Structural and conductivity studies on Lanthanum doped LiNiPO₄ prepared by polyol method*. World Scientific Publishing Co. Pte. Ltd.
- Komarov, V., Wang, S. and Tang, J. 2005. *Permittivity and Measurements*. Encyclopedia of RF and Microwave Engineering. John Wiley & Sons, Inc.
- Laskowski, J.J., Young, J., Gray, R., Acheson, R., Forder, S.D. (1994). The identity, development and quantification of phases in devitrified, commercial-grade, aluminosilicate, refractory ceramic fibres: an x-ray powder diffractometry study. *Analytica Chimica Acta* 286: 9-23.
- Leal, S.H., Escote, M.T., Pontes, F.M., Leite, E.R., Joya, M.R., Pizani, P.S., Longo, E., Varela, J.A. (2009). Structural transition on Pb_{1-x} Sr_xTiO₃ produced by chemical method. *Journal of Alloys and Compounds*, 475: 940–945.
- Lee, S.J., Thiyagarajan, P., Lee, M.J. (2008). Synthesis and characterization of strontium titanate powder via a simple polymer solution route. *Journal of Ceramic Processing Research*. 9(4): 385-388.
- Leow, C.Y., Hassan, J., Hashim, M., Wong, S.Y., Tan, F.K., Jeng, Wong, Y.J. (2011). Effect of Sintering Temperatures on the Microstructure and Dielectric Properties of SrTiO₃. *World Applied Sciences Journal*, 14 (7): 1091-1094.
- Li, J., Luo, S., Alim, M.A. (2006). The role of TiO₂ powder on the SrTiO₃-based synthesized varistor materials. *Materials Letters* 60: 720–724.
- Liu, H., X., Sun, Zhao, Q., Xiao, J., Ouyang S. (2003). The syntheses and microstructures of tabular SrTiO₃ crystal. *Solid-State Electronics*, 47: 2295–2298.
- Liu, T., Fothergill, J., Dodd, S., Nilsson, U. (2009). Dielectric spectroscopy measurements on very low loss cross-linked polyethylene power cables. *Journal of Physics: Conference Series*. 183: 012002.
- Loehman, R.E., Fitzpatrick, L.E. (1993). *Characterization of ceramics*. Butterworth-Heinemann.

- Mao, C., Yan, S., Cao, S., Yao, C., Cao, F., Wang, G., Dong, X., Hu, X., Yang, C. (2014). Effect of grain size on phase transition, dielectric and pyroelectric properties of BST ceramics. *Journal of the European Ceramic Society* 34: 2933–2939.
- Mitchell, B. S. (2003). *An introduction to materials engineering and science for chemical and materials engineers*. John Wiley & Sons, Inc.
- Morán, O., Hott, R., Fuchs, D. (2009). Study of SrTiO₃ thin films grown by sputtering technique for tunnel barriers in quasiparticle injection contacts. *Thin Solid Films* 517: 1908–1916.
- Moulson, A.J., Herbert, J.M. (1990). *Electroceramics : Materials, Properties, Application*. Chapman & Hall, 2-6 Boundary Row, London SE1 8H, UK.
- Naceur, H., Megriche, A., Maaoui, M. E. (2013). Frequency-dependant dielectric characteristics and conductivity behaviour of Sr_{1-x}(Na_{0.5}Bi_{0.5})_xBi₂Nb₂O₉ (x = 0.0, 0.2, 0.5, 0.8 and 1.0) ceramics. *Oriental Journal of Chemistry* 29 (3): 937-944.
- Naga, S.A.R., Naga, S.M.H., Mokhtar, M.O.A. (1992). Frictional behaviour of alumino-silicate ceramics. *Friboley International* 25: 2.
- Naghizadeh, R., Golestani-fard, F., Rezaie, H.R., (2011) Stability and phase evolution of mullite in reducing atmosphere. *Materials characterization* 62: 540 – 544.
- Nalwa, H.S. (Eds). (2001). *Handbook of advanced electronic and photonic materials and devices*. Elsevier Inc.
- Nautiyal, O.P., Bhatt, S.C., Pant, R.P., Semwal, B.S. (2010). Dielectric properties of silver sodium niobate mixed ceramic system. *Indian Journal of Pure & Applied Physics* 48: 357-362.
- Nussbaum, A. (1967). *Electronic and Magnetic Behaviour of Materials*. Prentice-Hall, China.
- Pamouch, R. (1991). *Constitution and Properties of Ceramics Materials*. PWN Polish Scientific Publishers, Warszawa.
- Pankratz, L.B., Weller, W.W., Kelley, K.K. (1963). Low-temperature heat capacity and high-temperature heat content of mullite. United State Department of the Interior. Bureau of Mines.
- Ring, T.A. (1996). *Fundamentals of Ceramic Powder Processing and Synthesis*. Elsevier Inc.
- Piva, R.H., Vilarinho, P., Morelli, M.R., Fiori, M.A., Montedo, O.R.K. (2013). Influence of Fe₂O₃ content on the dielectric behavior of aluminous porcelain insulators. *Ceramics International* 39: 7323–7330.

- Rosenberg, H. M. (1978). *The Solid State, Second Edition*. Oxford University Press.
- Roy, D., Bagchi, B., Das, S., Nandy, P., (2013). Electrical and dielectric properties of sol-gel derived mullite doped with transition metals. *Materials Chemistry and Physics* 138: 375-383.
- Roy, P.K., Bera, J. (2005). Formation of SrTiO₃ from Sr-oxalate and TiO₂ Materials. *Research Bulletin* 40: 599–604.
- Sainz, M.A., Serrano, F.J. Amigo, J.M., Bastida, J., Caballero, A. (2000). XRD microstructural analysis of mullites obtained from kaolinite-alumina mixtures. *Journal of the European Ceramic Society*, 20: 403-412.
- Sanad, M.M.S., Rashad, M.M., Abdel-Aal, E.A., El-Shahat, M.F. (2013). Mechanical, morphological and dielectric properties of sintered mullite ceramics at two different heating rates prepared from alkaline monophasic salts. *Ceramics International*, 39:1547–1554.
- Schneider, H., Komarneni, S. (2005). *Mullite*. Wiley-VCHnVerlag GmbH & Co. KGaA Weinheim.
- Schneider, H., Schreuer, J., Hildmann, B. (2008). Structure and properties of mullite—A review. *Journal of the European Ceramic Society*, 28: 329–344.
- Shaban, S.M., Mahdi, Bushra S Al-Haddad (2013) AC conductivity and dielectric behaviour of CuZnSnO₄ compound prepared by powder technology. *Indian Journal of Pure & Applied Physics* 51: 784-787.
- Shaikh, P.A. Kambale, R.C., Rao, A.V., Kolekar, Y.D. (2009). Comparative studies on structural and electrical properties of lead titanate synthesized by ceramic and co-precipitation method. *Journal of Alloys and Compounds*. 486: 442–446.
- Shkabko, A., Aguirrea, M.H., Marozub, I., Doebeli, M., Mallepell, M., Lippert, T., Weidenkaff, A. (2009). Characterization and properties of microwave plasma-treated SrTiO₃. *Materials Chemistry and Physics*, 115: 86–92.
- Sidebottom, D.L., Green, P.F., Brow, R.K. (1995). Comparison of KWW and power law analyses of an ion-conducting glass. *Journal of Non-Crystalline Solids* 183:151-160.
- Sikalidis, C. (2009) *Advances in ceramics - Synthesis and characterization, processing and specific applications*. InTech.
- Singh, A.K., Barik, S. K., Choudhary, R. N. P., Mahapatra, P. K. (2009). AC conductivity and relaxation mechanism in Ba_{0.9}Sr_{0.1}TiO₃. *Journal of Alloys and Compounds* 479: 39-42.
- Singh, D., Lorenzo, M. M., Chen, G., Gutierrez-Mora , F. Routbort , J.L. (2007). High-temperature deformation behavior in SrTiO₃ ceramics. *Journal of the European Ceramic Society* 27: 3377–3384.

- Somiya, S., Aldinger, F., Spriggs, K., Uchino, R., Koumoto, K., Kaneno, M. (2003). *Handbook of Advanced Ceramics*, Elsevier Inc.
- Teranishi, T., Hoshina, T., Tsurumi, T. (2009). Wide range dielectric spectroscopy on perovskite dielectrics. *Materials Science and Engineering B* 161 55–60.
- Thakur, O.P., Kumar, D., Parkash, O., Pandey L. (2003). Electrical characterization of strontium titanate borosilicate glass ceramics system with bismuth oxide addition using impedance spectroscopy. *Materials Chemistry and Physics* 78: 751–759.
- Tkach, A., Vilarinho, P. M., Kholkin, A. L. (2005). Structure–microstructure–dielectric tunability relationship in Mn-doped strontium titanate ceramics. *Acta Materialia* 53: 5061–5069.
- Tilley, R. J. D. (2004). *Understanding Solids: The Science of Materials*. John Wiley & Sons Ltd, The Atrium, Southern Gate, Chichester, West Sussex PO19 8SQ, England.
- Vermaa, K.C., Kotnalab, R.K., Mathpalb, M.C., Thakura, N., Gautamc, P., Negi, N.S. (2008). Dielectric properties of nanocrystalline $\text{Pb}_{0.8}\text{Sr}_{0.2}\text{TiO}_3$ thin films at different annealing temperature. *Materials Chemistry and Physics* 114: 576-579.
- Wang, T.X., Chen, W.W. (2008). Solid phase preparation of submicron-sized SrTiO_3 crystallites from SrO_2 nanoparticles and TiO_2 powders. *Materials Letters* 62: 2865–2867.
- Wang, Z., Cao, Mi., Yao, Q., Zhang, Z., Song, Z., Hu, W., Xu, Q., Hao, H., Liu, H., Yu., Z. (2014). Giant permittivity and low dielectric loss of SrTiO_3 ceramics sintered in nitrogen atmosphere. *Journal of the European Ceramic Society* 34: 1755–1760.
- Whitney, D.L. (2002). Coexisting andalusite, kyanite, and sillimanite: Sequential formation of three Al_2SiO_5 polymorphs during progressive metamorphism near the triple point, Sivrihisar, Turkey. *American Mineralogist* 87 (4): 405–416.
- Whittaker, E.J.W. (1981). *Crystallography an introduction for earth science (and other solid state) students*. Pergamon Press Ltd.
- Wong, S.Y., Hassan, J., Hashim, M. (2009). Dielectric properties of strontium titanate in the 1 MHz To 1.5 GHz frequency regions. *Solid State Science and Technology* 17(1): 57 – 62.
- Wong, Y.J. (2013) *Dielectric properties of Strontium Titanate and Calcium Titanate prepared via solid state and mechanical alloying methods*. (Unpublished master's thesis). Universiti Putra Malaysia, Malaysia.
- Xu, H., Wei, S., Wang, Zhu, H.M., Yu, R., Yan., H. (2006). Preparation of shape controlled SrTiO_3 crystallites by sol–gel-hydrothermal method. *Journal of Crystal Growth*, 292: 159–164.

Xu, Y. (1991). *Ferroelectric Materials and their Applications*. North Holland. Amsterdam.

Young, K.F., Frederikse, H.P.R. (1973) Compilation of the static dielectric constant of inorganic solids. *Journal of Physical and Chemical Reference Data* 2(2): 313-410.

Yu, J., Shi, J.-L., Yuan, Q.-M., Yang, Z.-F., Chen, Y.-R. (2000). Effect of composition on the sintering and microstructure of diphasic mullite gels. *Ceramics International*, 26 : 255–263.

Zaki H.M. (2005). AC conductivity and frequency dependence of the dielectric properties for copper doped magnetite. *Physica B* 363: 232–244.

Zhao, J., Wu, X., Li, L., Li, X. (2004). Preparation and electrical properties of SrTiO₃ ceramics doped with M₂O₃–PbO–CuO. *Solid-State Electronics* 48: 2287–2291.